

Antibacterial Activities of Titanium Oxide Nanoparticles

Keywords: TiO₂ nanorods; Optical properties; Microwave assisted; Antibacterial activity

Abstract

Titanium dioxide nanostructures are promising material for optical and antibacterial applications. In this study, TiO₂ nanoparticles have been synthesized using facile microwave-assisted hydrothermal process. The optical properties and the structure of the synthesized TiO₂ nanoparticles were characterized using several techniques such as Transmission Electron Microscopy (TEM), UV measurements, Fourier Transform Infrared (FTIR), Energy and Dispersive X-ray Spectroscopy (EDXS), X-ray diffraction, Scanning Electron Microscopy (SEM), and Thermogravimetric (TGA). The antibacterial activity of TiO₂ nanoparticles were assessed against the pathogenic strain *E. coli* ATCC® 8739™. The reported results indicated superior antibacterial activity of TiO₂ nanoparticles tested against the pathogenic bacteria, which reveals potential applications of TiO₂ nanoparticles in biomedical and medical fields.

Introduction

Photocatalysis is essentially an advanced oxidation process, which has proved to be an effective approach to degrade a wide range of organic, inorganic compounds and toxic metal ions, and to kill microorganisms and viruses. In addition, photocatalysis is an entirely green technology, which does not require or consume any chemical additives (some photocatalytic applications involve other oxidants such as hydrogen peroxide H₂O₂ to enhance the efficiency). Thus, this emerging technology has demonstrated great promise for environmental applications such as water treatment and air purification. In the recent years, photocatalysis has been employed for water treatment to remove organic and inorganic molecules from water and gas. Fujishima et al. reported that photocatalysis is able to divide water into hydrogen and oxygen [1]. ZnO, Fe₂O₃, MgO, WO₃, Bi₂WO₆, Bi₂O₃ and TiO₂ are the most semiconductors that can be used for photocatalysis and safe materials for human beings, animals and plants [2]. These attractive features enable these materials to be applied in different applications such as chemical sensors, medicine and water treatment. Recently Hunge et al. have prepared tungsten trioxide (WO₃) thin films using spray pyrolysis technique and used it for the degradation of methyl orange. They reported that the degradation rate of methyl orange was over 98% using WO₃ photoelectrodes which confirms that it can be employed for applications of water purification [3].

Titanium dioxide (TiO₂) nanoparticles have been commonly employed as photocatalysts because TiO₂ is biologically and chemically stable, corrosion-resistive and inexpensive [4]. TiO₂ is abundance in nature, non-toxic with great optical transparency and refractive index and wide band gap energy [5]. One dimensional TiO₂ nanostructures with different morphologies prepared by different techniques, such as nanorods, nanowires and nanotubes structures [6-9]. In recent years, TiO₂ nanostructures have been synthesized using various methods such as sol-gel, hydrothermal, solvothermal,

pulsed laser deposition, Chemical Vapor Deposition (CVD), electrodeposition, Microwave method, spray pyrolysis and sputtering [5,10-14]. Among these methods, spray pyrolysis technique has been widely used for several environmental applications [5]. TiO₂-activated carbon nanocomposite was synthesized using a sol-gel method to study photocatalytic degradation of reactive red 198, and it was reported that nanocomposite enhanced the photocatalytic activity of TiO₂ nanoparticles [4]. Hunge et al. have prepared stratified WO₃/TiO₂ thin films and reported that the film can be used for treatment of polluted water [4]. Microwave heating method is attractive due to its capability of generating fast bulk heating which can result in high reaction rates during short reaction time, and massive product yield in comparison with conventional heating technologies [15-19]. Hence, microwave technology is a promising technology for the development of the green chemistry and it is an essential technology for synthesizing of nanostructures with versatile morphology and uniform particle size [20-27].

Wound infection is considered as a global problem of human health and contributes significantly to the escalation in the cost of health care [28]. Wound infection is classified as acute or chronic based on the natural repair process [29]. Antibiotics are the most preferred therapeutic agent to treat and prevent wound infection [28]. Although antibiotics are effective in treating the bacterial infection, improper use of antibiotics creates multidrug resistance microorganisms [30]. Increase prevalence of antibiotic resistance with less development in the antibiotic field resulting in the shortage of novel classes of the antibiotic agent that used to eliminate multidrug-resistant bacteria [31]. In recent years, researchers start to look for the alternative safe treatment which can be employed instead of conventional antibiotic for wound infection. Currently, there are some noble metallic nanoparticles have an effective antibacterial



Hani A. Alhadrami^{1,2*} and Faten Al-Hazmi³

¹Faculty of Applied Medical Sciences, Department of Medical Laboratory Technology, King Abdulaziz University, Kingdom of Saudi Arabia.

²Special Infectious Agents Unit, King Fahd Medical Research Center, King Abdulaziz University, Kingdom of Saudi Arabia

³Department of Physics, King Abdulaziz University, Kingdom of Saudi Arabia

*Address for Correspondence

Hani A. Alhadrami, Faculty of Applied Medical Sciences, Department of Medical Laboratory Technology and Special Infectious Agents Unit, King Fahd Medical Research Centre, King Abdulaziz University, P. O. Box 80402, Jeddah, 21589, Kingdom of Saudi Arabia, Tel: +966505545275; E-mail: haniahadrami@kau.edu.sa

Submission: 26 February, 2017

Accepted: 22 March, 2017

Published: 28 March, 2017

Copyright: © 2017 Alhadrami HA, et al. This is an open access article distributed under the Creative Commons Attribution License, which permits unrestricted use, distribution, and reproduction in any medium, provided the original work is properly cited.

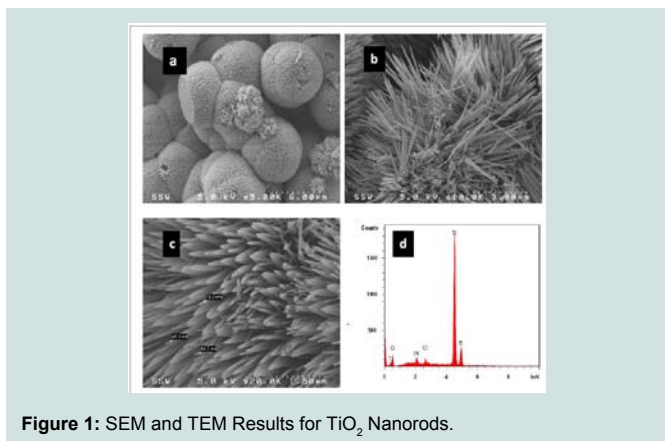


Figure 1: SEM and TEM Results for TiO₂ Nanorods.

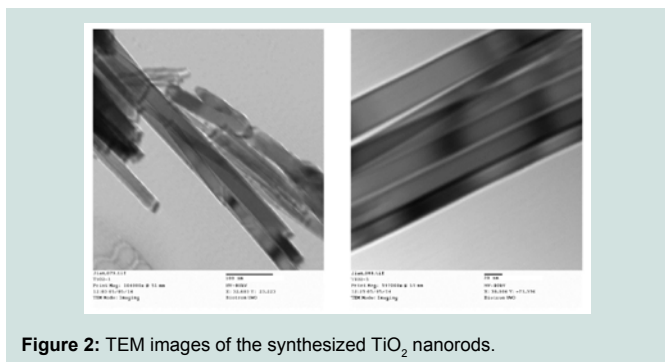


Figure 2: TEM images of the synthesized TiO₂ nanorods.

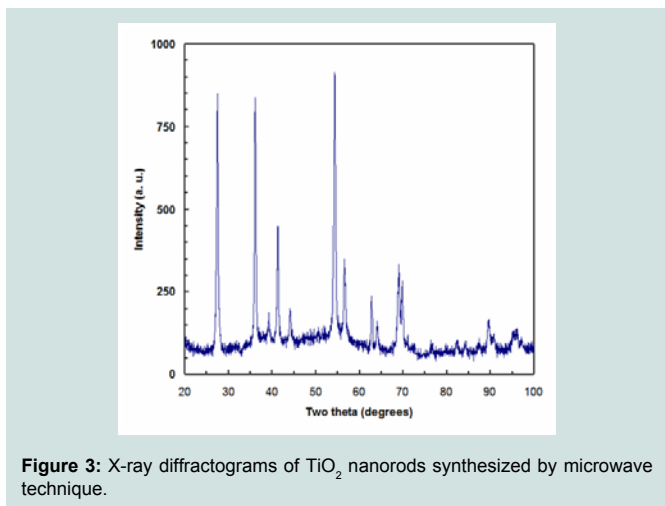


Figure 3: X-ray diffractograms of TiO₂ nanorods synthesized by microwave technique.

activity such as zinc, copper, titanium and silver [30,31]. One of the most attractive nanoparticles that can be used for the treatment of wound infection is titanium dioxide (TiO₂) nanoparticles [27]. TiO₂ nanoparticles have been recently employed in medical applications due to their attractive features such as versatile surface chemistry, highly controllable absorption, improve tissue penetration and reduce photochemical damage [2]. Introducing novel TiO₂ nanoparticles as antibacterial agents can control the mortality and morbidity rate of the infectious diseases.

In this study, we synthesized TiO₂ nanorods using a facile

microwave-assisted hydrothermal process taking into consideration several parameters such as, time, temperature, and concentration of basic solution on the growth of nanocrystals. The structural of the produced nanoparticles have been characterized using XRD, SEM, EDS, FTIR, UV and TEM. Optical, thermal and antibacterial properties of TiO₂ nanorods were addressed in detail.

Materials and Methods

Synthesis of TiO₂ nanorods

TiO₂ nanorods have been synthesized using wet chemical process with microwave-assisted. Two chemical processes were used to control the synthesis of TiO₂ nanorods. The first was a wet chemical route assessment of microwave irradiation and hydrothermal technique. The second was based on a simple reaction with water to synthesis the proposed TiO₂ nanorods. The synthesis process involved using 25 ml of Titanium (IV) tetrachloride tetrachloride (TiCl₄, 99.9%, purchased from Aldrich), and 50 ml of water. Microwave hydrothermal technique was used as follows: Titanium tetrachloride was mixed with distilled water. The mixture was transferred into Teflon-lined autoclave. The autoclave was sealed and maintained to 220 °C for 90 min in microwave furnace with a power 700 w, then left to cool down at room temperature. Precipitates were collected by centrifugation at 3000 rpm for 5 min, and then a nomination with distilled water was applied to reduce the agglomeration. The mixture was dried at 80 °C for 3 h and the white powder of TiO₂ nanorods was finally generated.

Antibacterial activity of TiO₂ nanorods

E. coli ATCC[®] 8739[™] was grown overnight in 250 ml Erlenmeyer flask containing 100 ml Luria Bertani (LB) broth, and incubated in 150 rpm orbital shaker incubator at 37 °C. The overnight culture was harvested by centrifugation at 6000 rpm for 5 minutes. To remove any bound organic and inorganic components, the cells were washed twice with normal saline (0.85% NaCl solution at pH 6.5). The washed cells were re-suspended in 4 ml normal saline. TiO₂ nanorods were washed with 70% ethanol and left to dry for 5 min. The bacterial suspension was incubated with 100 mg TiO₂ nanorods and incubated overnight at 37 °C in 150 rpm orbital shaker incubator. An aliquot (100 µl) was taken at different time intervals (0, 30 min and 24 h), diluted and plated on LB agar plates to determine the number of colony forming units (CFUs/ml). Counts of CFUs were performed by applying the drop-plate method. Serial dilutions (1:10) were achieved by diluting the bacterial cells (100 µl) in micro-centrifuge tubes containing 25% normal saline (900 µl). Three 10 µl aliquots of the appropriate dilution were spotted onto LB agar plate and incubated overnight at 37 °C. The experiment was performed in triplicate, and negative control (TiO₂ nanorods incubated with LB broth) was used.

Results and Discussion

SEM and TEM results of TiO₂ nanorods

Size and morphology of the synthesized TiO₂ nanorods were examined by SEM. High and low SEM magnification images are illustrated in (Figures 1a and 1b) respectively. It is clearly noticeable in (Figure 1c) that the obtained products have been successfully synthesized in large quantity and retaining nanorod-like morphologies. EDS spectra of the synthesized TiO₂ nanorods was represented in (Figure 1d), which indicated the existence of oxygen

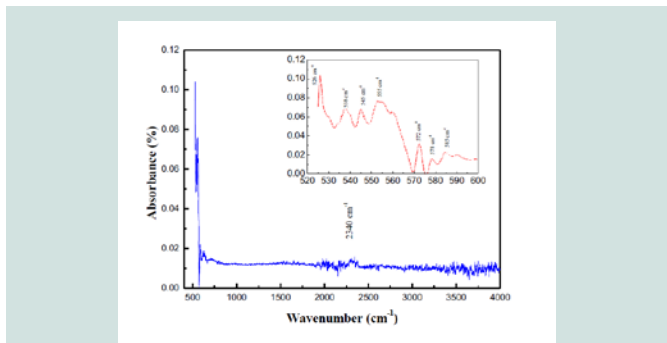


Figure 4: FTIR spectra of TiO₂ nanorods synthesized by microwave technique.

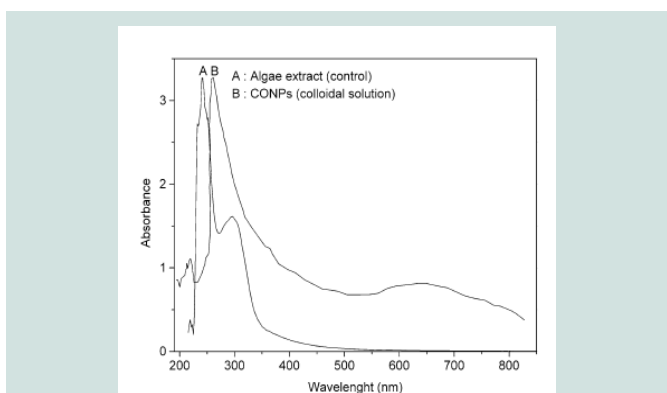


Figure 5: Plots of versus $(\alpha h\nu)^2$ for TiO₂ nanorods.

and Mg. TME was used to demonstrate the clear morphologies of the synthesized TiO₂ nanorods (Figure 2). The results confirmed that the TiO₂ had uniform nanorods and are grown in large scale.

X-ray studies of TiO₂ nanorods

The typical X- ray diffraction pattern of TiO₂ nanorods synthesized by microwave technique is presented in (Figure 3). The X- ray diffraction pattern confirmed that TiO₂ had a polycrystalline structure. The significant peaks for the pristine TiO₂ were observed at 2=27.62°, 36.21°, 38.37°, 41.37°, 44.60°, 54.45°, 56.85°, 63.05°, 65.06° and 69.17°, which could be indexed as (110), (101), (200), (111), (210), (211), (220), (002), (310) and (301), respectively based on JCPDS card No. 01-089-4920. The peaks are fully assigned to TiO₂ and their broad width suggests the presence of small-sized particles. The crystal structure of the TiO₂ is rutile tetragonal structure with lattice parameter of a=0.4512 nm and c=0.2943 nm. The average size of crystallites was determined based on X-ray peak broadening the (101) reflection using the Scherrer formula:

$$D = \frac{0.9\lambda}{\beta \cos \theta} \tag{1}$$

Where D is the average dimensions of crystallites, β is the broadening of the diffraction line measured at half maximum intensity, λ is the wave length of the x-ray radiation and θ is the Bragg angle. Based on peak broadening (Figure 3), the calculated crystallite size of as prepared TiO₂ is found to be of the order of 17 nm.

Fourier Transformation Spectroscopy (FTIR) analysis

FTIR spectroscopy was used in the range of 400–4000 cm⁻¹ to assess the chemical composition and the quality of the synthesized TiO₂ nanoparticles. FTIR spectrum results of the synthesized TiO₂ nanorods were presented in (Figure 4). The results showed the

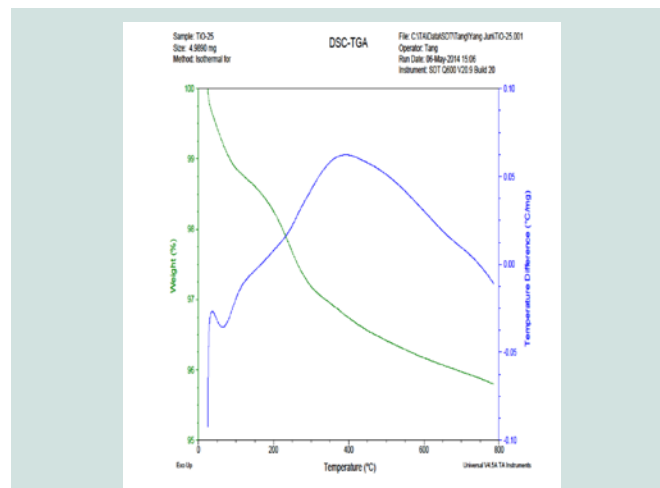


Figure 6: TGA curve in air for the synthesized TiO₂ nanorods.

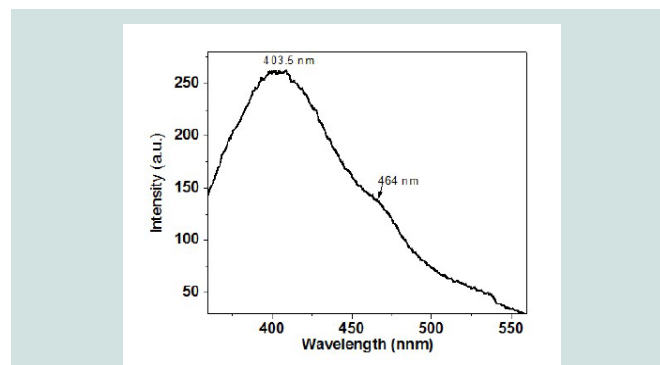


Figure 7: Photoluminescence for synthesized TiO₂ nanorods.

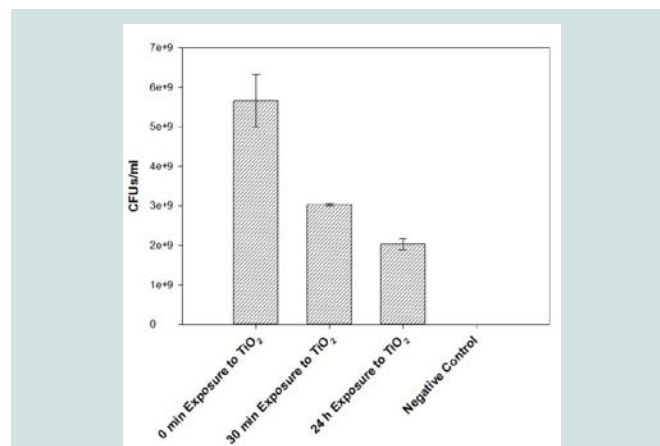


Figure 8: Antibacterial activity of TiO₂ nanorods tested against E. coli ATCC® 8739™ at different time intervals.

presence of sharp and strong two bands at 526 and 585 cm^{-1} . This was due to the formation of the stretching vibration of metal-oxygen (Ti-O) bonds. This reveals that the synthesized products were pure TiO_2 . Further, the presence of a band located at 2340 cm^{-1} was due to the characteristic absorption of TiO_2 . In summary, the FTIR spectra confirmed that the synthesized TiO_2 nanoparticles composed of one phase, which agrees with X-ray analysis.

Optical properties of TiO_2 nanorods

The energetic bands structure and the energy band gap of the prepared TiO_2 nanorods have been determined using optical absorption spectra. The absorption coefficient (α) is related to the band gap (E_g) by the following equation (Assuming the band gap to be parabolic in nature):

$$(\alpha h\nu)^2 = B(h\nu - E_g)^n \quad (1)$$

Where (h) is the plank constant, (ν) is the photo frequency, (B) is a constant and (n) is the transition type. The absorption coefficient (α) can be extracted from:

$$I = I_0 e^{-\alpha t} \quad (2)$$

Where (I) is the intensity of transmitted light, (I_0) is the intensity of the incident light, and (t) is the thickness of the sample.

The optical band gap (E_g) of the synthesized TiO_2 nanorods was calculated from plotting ($\alpha h\nu$) versus ($h\nu$) as illustrated in (Figure 3). The linearity of plotting ($\alpha h\nu$)² on the y-axis versus ($h\nu$) on the x-axis was interpolated to cut x-axis corresponding to $y = 0$. The intercept on the x-axis is a measure of the E_g of the tested samples. As seen in (Figure 5), the optical band energy gap is about 2.3 eV.

TGA analysis

The Thermogravimetric (TGA) analysis of the synthesized TiO_2 was presented in (Figure 6). The results confirmed two distinctive weight loss steps (Figure 6). The first weight loss happened at 100-250 $^\circ\text{C}$, which paralleled to the evaporation of crystallized water. The second weight loss took place at around 260-700 $^\circ\text{C}$, leading to the conversion of anhydrous titanium to titanium oxide.

Photoluminescence spectroscopy

Previously reported results showed that the indirect gap nanostructure semiconductors can have luminescence because of quantum confinement. Accordingly, many researchers were directed to explore the optical and optoelectronic properties of indirect gap nanostructures. Figure 7 showed photoluminescence measured at room temperature excited by energy chosen at the wavelength corresponding to the position of the minimum appeared in the first derivative of absorption spectrum. The luminescence spectrum of the nanotube consists of high energy emission in blue region of visible light with high intensity at 404 nm along with low intensity shoulder at 464 nm. The emission at 404 nm was at energy slightly less than the value of the determined band edge, which could be attributed to free excitons near to the band edge. The low intensity shoulder at 464 nm may be attributed to Ti-OH complex existing at the surface of nanotube, which induces surface states in the band gap of nanotubes.

Antibacterial activity of TiO_2 nanorods

The antibacterial activity of TiO_2 nanorods tested against *E. coli* ATCC[®] 8739[™] is presented in (Figure 8). The viable bacteria were monitored by counting the number of Colony Forming Units (CFUs). The presented results are an average of triplicate measurements and a negative control (TiO_2 nanorods incubated with LB broth). Statistical analysis was performed using Minitab 15 for Windows to compare the number of CFUs/ml during different exposure time to TiO_2 nanorods (0, 30 min and 24 h). The results revealed a significant reduction ($p < 0.05$) in the number of CFUs/ml after only 30 min of exposure to TiO_2 nanorods (Figure 8). There was a significant difference between the number of CFUs/ml after 0 min exposure to TiO_2 nanorods and the number of CFUs/ml after 30 min exposure. A growth inhibition of three orders of magnitude is observed after only 30 min of exposing *E. coli* to the TiO_2 nanorods. Further, a significant decrease ($p < 0.05$) is observed in the number of CFUs/ml for *E. coli* after 24 h exposure to the TiO_2 nanoparticles (Figure 8). Taken together these results, there was superior antibacterial activity of the synthesized TiO_2 nanorods against the pathogenic bacteria *E. coli*, which demonstrates potential applications of TiO_2 nanorods in medical and biomedical fields.

Conclusion

In this work, performance photocatalysts TiO_2 nanorods were successfully synthesized using microwave-assisted hydrothermal process. The SEM, EDX, TEM and XRD analysis indicated that photocatalysts TiO_2 nanorods are crystalline. Moreover, photocatalysts TiO_2 nanorods using water as a solvent via a facile microwave-assisted hydrothermal process were prepared in this work for the first time. The TiO_2 nanorods have an effective antibacterial ability against *Escherichia coli* (Gram negative), which makes TiO_2 nanorods very useful as antibacterial agent and in many biomedical applications. Finally, the one outstanding feature of this study is that we need more experimental work under different growth conditions to which we could demonstrate that photocatalysts metal oxide nanostructures are promising for important applications in water purification.

References

1. Fujishima A, Honda K (1972) Electrochemical photolysis of water at a semiconductor electrode. Nature 238: 37-38.
2. Wang M, Iocozzi J, Sun L, Lin C, Zhiquan Lin (2014) Inorganic-modified semiconductor TiO_2 nanotube arrays for photocatalysis. Energy Environ Sci 7: 2182-2202.
3. Hunge YM, Mahadik MA, Kumbhar SS, Mohite VS, Rajpure KY et al. (2016) Visible light catalysis of methyl orange using nanostructured WO_3 thin films. Ceram Int 42: 789-798.
4. Hunge YM, Mahadik MA, Moholkar AV, Bhosale CH (2017) Photoelectrocatalytic degradation of oxalic acid using WO_3 and stratified WO_3/TiO_2 photocatalysts under sunlight illumination. Ultrason Sonochem 35(Pt A): 233-242.
5. Mohite VS, Mahadik MA, Kumbhar SS, Hunge YM, Kim HJ, et al. (2015) Photoelectrocatalytic degradation of benzoic acid using Au doped TiO_2 thin films. J Photochem Photobiol B 142: 204-211.
6. Varghese OK, Gong D, Paulose M, Ong KG, Dickey EC, et al. (2003) Extreme changes in the electrical resistance of titania nanotubes with hydrogen exposure. Adv Mater 15: 624-627.
7. Wen B, Liu C, Liu Y (2005) Depositional characteristics of metal coating on

- single-crystal TiO₂ nanowires. J Phys Chem B 109: 12372-12375.
8. Wu JM, Qi B (2007) Low-temperature growth of a nitrogen-doped titania nanoflower film and its ability to assist photodegradation of rhodamine B in water. J Phys Chem C 111: 666-673.
 9. Yi GR, Moon JH, Yang SM (2001) Ordered macroporous particles by colloidal templating. Chem Mater 13: 2613-2618.
 10. Andersson M, Oesterlund L, Ljungstroem S, Palmqvist A (2002) Preparation of nanosize anatase and rutile TiO₂ by hydrothermal treatment of microemulsions and their activity for photocatalytic wet oxidation of phenol. J Phys Chem B 106: 10674-10679.
 11. Wahi RK, Liu Y, Falkner JC, Colvin VL (2006) Solvothermal synthesis and characterization of anatase TiO₂ nanocrystals with ultrahigh surface area. J Colloid Interface Sci 302: 530-536.
 12. Bazargan MH, Byranvand MM, Kharat AN (2012) Preparation and characterization of low temperature sintering nanocrystalline TiO₂ prepared via the sol-gel method using titanium (IV) butoxide applicable to flexible dye sensitized solar cells. Int J Mat Res 103: 347-351.
 13. Shinde PS, Bhosale CH (2008) Properties of chemical vapour deposited nanocrystalline TiO₂ thin films and their use in dye-sensitized solar cells. J Anal Appl Pyrolysis 82: 83-88.
 14. Arami H, Mazloumi M, Khalifehzadeh R, Sadrnezhaad SK (2007) Sonochemical preparation of TiO₂ nanoparticles. Mater Lett 61: 4559-4561.
 15. Fang X, Zhang L (2006) One-dimensional (1D) ZnS nanomaterials and nanostructures. J Mater Sci Technol 22: 721-736.
 16. Cui Z, Meng GW, Huang WD, Wang GZ, Zhang LD (2000) Preparation and characterization of MgO nanorods. Mater Res Bull 35: 1653-1659.
 17. Yin Y, Zhang G, Xia Y (2002) Synthesis and characterization of MgO nanowires through a vapor-phase precursor method. Adv Funct Mater 12: 293-298.
 18. Zhang J, Zhang L, Peng X, Wang X (2001) Fabrication of MgO nanobelts using a halide source and their structural characterization. Appl Phys A 73: 773-775.
 19. Shah MA, Haq Q (2009) J Alloys Compd 442: 548.
 20. Al-Hazmi F, Umar A, Dar GN, Al-Ghamdi AA, Al-Sayari SA, et al. (2012) Microwave assisted rapid growth of Mg(OH)₂ nanosheet networks for ethanol chemical sensor application. J Alloys Compd 519: 4-8.
 21. Umar A, Al-Hazmi F, Dar GN, Zaidi SA, Al-Tuwirqi RM, et al. (2012) Ultra-sensitive ethanol sensor based on rapidly synthesized Mg(OH)₂ hexagonal nanodisks. Sens Actuators B Chem 166-167: 97-102.
 22. Beall GW, Duraia EM, El-Tantawy F, Al-Hazmi F, Al-Ghamdi AA (2013) Rapid fabrication of nanostructured magnesium hydroxide and hydromagnesite via microwave-assisted technique. Power Technol 234: 26-31.
 23. Al-Ghamdi AA, Al-Hazmi F, Alnowaiser F, Al-Tuwirqi RM, Al-Ghamdi AA (2012) A new facile synthesis of ultra fine magnesium oxide nanowires and optical properties. J Electroceram 29: 198-203.
 24. Aal NA, Al-Hazmi F, Al-Ghamdi AA, Al-Ghamdi A, El-Tantawy F, et al. (2015) Novel rapid synthesis of zinc oxide nanotubes via hydrothermal technique and antibacterial properties. Spectrochim Acta A Mol Biomol Spectrosc 135: 871-877.
 25. Al-Ghamdi AA, Al-Hazmi F, Al-Hartomy OA, El-Tantawy F, Yakuphanoglu F (2012) A novel synthesis and optical properties of cuprous oxide nano octahedrons via microwave hydrothermal route. J Solgel Sci Technol 63: 187-193.
 26. Al-Hazmi F, Alnowaiser F, Al-Ghamdi AA, Al-Ghamdi AA, Aly MM, et al. (2012) A new large-scale synthesis of magnesium oxide nanowires: structural and antibacterial properties. Superlattices Microstruct 52: 200-209.
 27. Al-Tuwirqi RM, Al-Ghamdi AA, Al-Hazmi F, Alnowaiser F, Al-Ghamdi AA, et al. (2011) Synthesis and physical properties of mixed Co₃O₄/CoO nanorods by microwave hydrothermal technique. Superlattices Microstruct 50: 437-448.
 28. Siddiqui AR, Bernstein JM (2010) Chronic wound infection: facts and controversies. Clin Dermatol 28: 519-526.
 29. Storm-Versloot MN, Vos CG, Ubbink DT, Vermeulen H (2010) Topical silver for preventing wound infection. Cochrane Database Syst Rev 17: CD006478.
 30. Aydin S, Ince B, Ince O (2016) Assessment of anaerobic bacterial diversity and its effects on anaerobic system stability and the occurrence of antibiotic resistance genes. Bioresour Technol, 207: 332-338.
 31. Kumari S, Harjai K, Chhibber S (2010) Evidence to support the therapeutic potential of bacteriophage Kpn5 in burn wound infection caused by *Klebsiella pneumoniae* in BALB/c mice. J Microbiol Biotechnol 20: 935-941.

Acknowledgements

The project was funded by Research Endowment Fund (WAQF), King Abdulaziz University, under grant 1435-1436. The authors, therefore, acknowledge with thanks WAQF financial support.